Automated, high-accuracy, remote measurement of heart rate

Yiming Yang, Yuliang Zhao*, Liming Xin*, and Yu Sun

Abstract. Arrhythmia is a marked symptom of many cardiovascular diseases. The accurate and in time detection of heart rate can greatly reduce its harm to people. However, it is still a challenge to automatedly and remotely measure the heart rate in daily life, because the environment factor of the measurement changes variously, such as the changing light intensity, the movement of people, and the uncertain distance from sensor to people. In this study, we accurately measured the heart rate of people at the distance of 4.8 meters under different intensity of light just by using a surveillance camera. After a short color video (20 sec) of a person's hand was captured by this camera, a method based on Fast Fourier Transform Algorithm (FFT) is proposed to extract the blood volume pulse wave to calculate the heart rate. By comparing the real heart rate with the results measured by electrocardiography (ECG), the accuracy of heart rate measurement using the method proposed in this study is 98.65% within 4.0 meters, and the accuracy can reach 90% within 5.6 meters. Our experiments also demonstrated that this method can accurately obtain the heart rate even when the intensity of light is below 32 LUX (office environment 300-500 LUX). The strong environmental suitability makes this method can be applied to many occasions, such as community clinic, old peoples' home, classroom, and other public space.

Key words: heart rate measurement; rPPG; non-contact; photoplethysmography; surveillance camera.

I. Introduction

Heart rate, an important parameter of a living body, plays a major role in personal fitness[1], electronic commerce[2], financial trading[3], and disease prediction[4]–[8]. Cardiovascular disease (CVD) is the leading cause of death today[9]–[11]. Around 17.9 million people died from CVD in 2016, representing 31% of all global deaths [12]. A large number of clinical studies have shown that irregular heart rate is a complication of cardiovascular diseases (such as coronary heart disease [4], hypertension [5] and heart failure [6]), and can used to predict the occurrence of cardiovascular diseases [7][8].

Frequent heart rate monitor has a great positive effect on the prevention of cardiovascular diseases. The traditional heart rate measurement method, electrocardiography (ECG), requires the

subject to stick electrodes on the body or wear a chest strap. ECG will cause certain irritation and discomfort to patients, moreover, the equipment is not portable enough, which is very inconvenient for most of scenes of life, such as home or office.

Smart bracelets for heart rate detection is another choice, where the Photoplethysmography (PPG) detection technology are often adapted. PPG is a non-invasive detection method that uses optical technology to detect changes in blood volume in living tissues, and is mainly used in pulse oximeters. In the measurement, it requires a specific light source or infrared wavelength light and a contact sensor probe. Although the comfort is improved compared with the traditional heart rate measurement method. However, the limitation of the battery make it cannot afford the long-term usage and multitasking capability, especially the frequently communication and calculation.

Currently, there are a large number of remote non-contact heart rate measurement methods have been developed, such as the methods based on thermal imaging [13] and microwave Doppler radar [14], which requires expensive and specialized hardware.

Remote photoplethysmography (rPPG) is a non-invasive, remote, low-cost measurement method. It uses a camera to collect the reflected light from the skin and analyze it to obtain heart rate. The existing rPPG method uses Independent component analysis (ICA) [15], Principal Component Analysis (PCA) [13], Butterworth pass band filter [16], Random Forest Regression (RFR) [17], and fast Fourier Transform (FFT) [18] [19] for heart rate measurement. All these methods always effectively detach the heart rate signals from the noises bring by the complicated environment and subjects. Therefore, the illumination robustness and the available distance of these types of detections are very limited. And the specific parameters of these methods are compared in Tab.1.

Tab.1 Comparation of different rPPG methods

Core algorithm	Shooting time /second	Research on brightness robustness Y/N	Research on illumination range Y/N	Measuring range /meter	Study
ICA	60	N	N	0.5	[15]
PCA	30	N	N	1	[13]
Butterworth pass band filter	60	N	N	<3	[16]
RFR	35	N	N	1	[17]
FFT	30	N	N	0.8-1	[18]
FFT	30	N	N	1-2	[19]
Filtering for blood color +FFT	20	Y	Y	<4.8	This study

From the table above, it is easy to find that there are two main problems of these methods. Firstly, the effective measuring distance is too short for a convenient detection of the heart rate. Secondly， the detection in poor lighting conditions and the drastic changes of the illuminance have not been fully studied.

In this study, we have proposed a method for heart rate detection using home surveillance cameras, which can detected the heart rate in the distance of 4.8 meters away from the person, and also can be applied to low-light environments and has light robustness. This outstanding performance lays on three special operations comparing to the other rPPG methods. Firstly, we found that the image processing operation by minus G channel from R channel of the image will eliminate most of the environment noisy. Which makes our method owns enough illumination robustness and cannot be affected by the change, when the illuminance change suddenly. And this point are supported by our the heart rate detecting experiments. Secondly, we used the FFT algorithm to filter a lot of environmental noise and calculate the heart rate. Using the above two algorithms, thirdly, through searching the strongest signal position on the skin, and setting this position as ROI , we greatly improved the measurement accuracy and extend the measurement distance. Which fully validated the noise eliminating ability of our method on the changes of illumination and distance. Finally, we use the method proposed above to measure the heart rate of ROI at a serial different distances and illuminances.

By reduce the no signal area and enhance the heart rate signal, this method successfully extended the detection distance. When the user appears in the shooting range of the camera, the system can detect the heart rate according to the subtle change of the user's skin color, and upload the data to the cloud for analysis. Which can be used to remind the patients suffering from

cardiovascular diseases to seek medical diagnosis in time. The method proposed in this study will be helpful on the maintaining human health and can be applied to many occasions to determine the possibility of a user suffering from cardiovascular disease by remotely monitoring the user's heart rate. Updating with a more powerful camera, it is reasonable to expect this method can be used to help the patients suffering from cardiovascular disease on many aspects (such as family health care, personal fitness, electronic commerce, and financial trading).

Ⅱ. Method

A. Experimental Protocol

The detection equipment used in this study consists of a 3-lead electrocardiogram (Texas Instruments' ADS1292) and an ordinary camera (Sony IMX345 sensor, F/2.4, 52mm, 1/3.6, 1 µm, AF). The camera worked at a frame rate of 60 frames/s. All videos were recorded in color space with a resolution of 1920 × 1080. During the measurement, the tester's hand is placed flat under the camera. The light intensity was measured by HABOTEST's HT620L in the experiments. In total, 5 healthy volunteers (three males and two females with the age of 47, skin color: Yellow) without any known cardiovascular diseases participated the experiment. Informed consent was obtained from each candidate. The vertical distance between the camera and the hand is less than 4.8 meters. To validate the proposed method, a 3-lead ECG was used to measure the people's heart rate synchronously. The acquired data are processed in MATLAB 2019A.

The subject sticks the electrodes of the ECG signal collector to the body part as shown in Fig.1 (ECG signal is used as benchmark). The subject puts his hand flat facing the camera. At the beginning of the experiment, the ECG signal collector and the camera are started at the same time to ensure that the time synchronization. The ECG signal collected by the ECG signal collector and the video captured by the camera are transferred to the computer for further analysis.

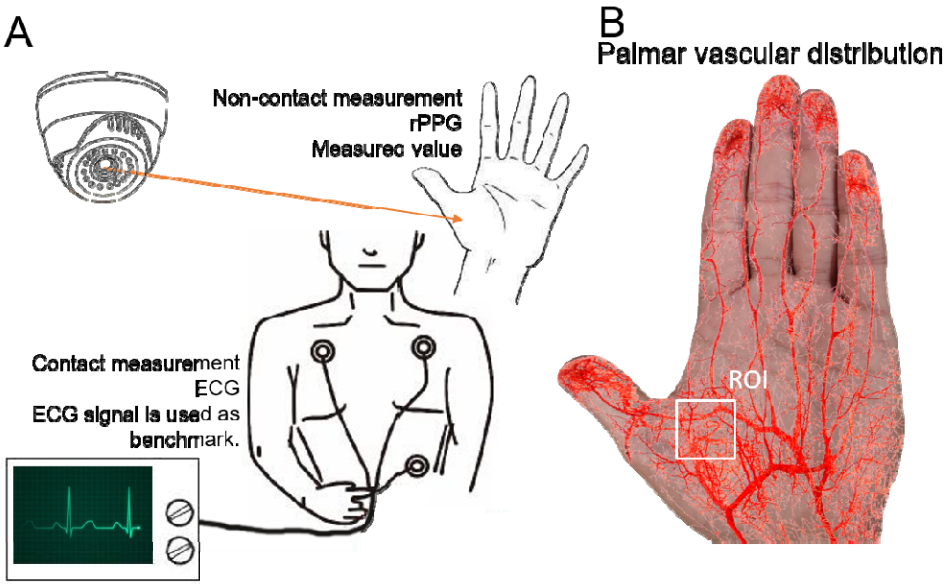

Fig.1 (**A**) Experimental diagram; (**B**) Blood vessel distribution in the palm

B. Fliting Noisy

After the camera shooting the video of the hand, the video was preprocessed to the image serials . Firstly, each frame of the video were saved as the image in matrix. Secondly, after recognizing the palm in the image, ROI were cut from the palm picture as shown in Fig.2. Although Fig.2A and Fig.2B are the two images with the largest color difference, it's still difficult to distinguish them only by the naked eyes. The signal-to-noise ratio (SNR) of this kind of image is too low to product a good heart rate detecting result, even based on the advantage algorithms.

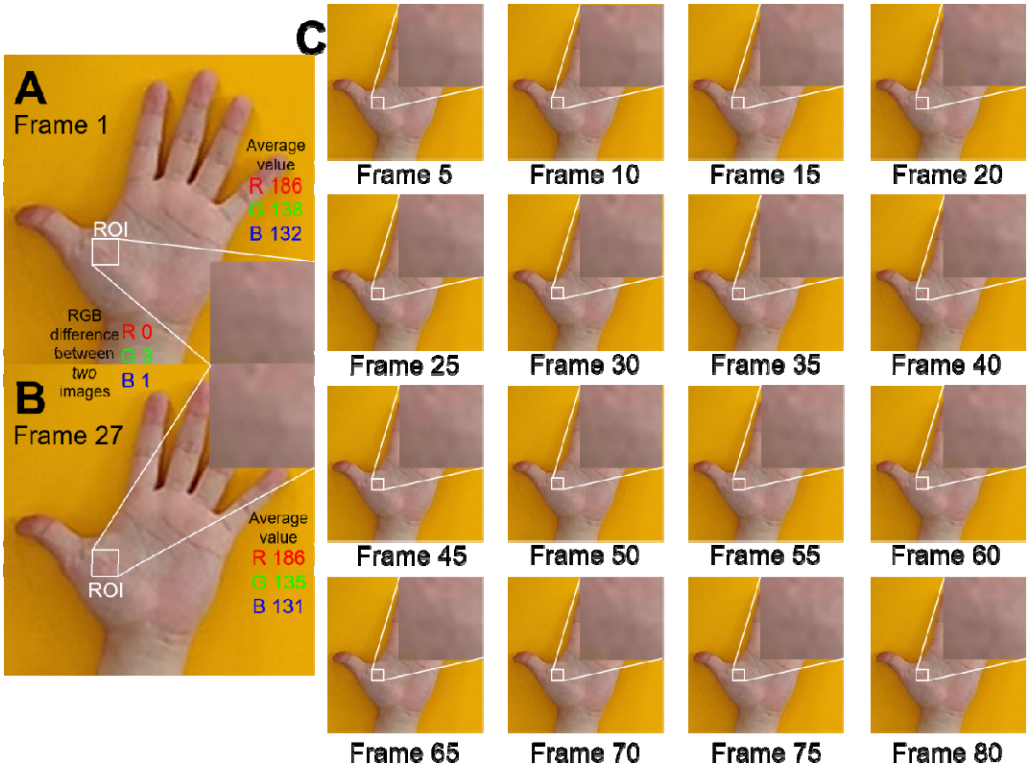

Fig.2 The images contrast between two frames (**A**-**B**); (**C**) The captured sequence images. The video is shot at 60 fps.

The main limitation of the kind of rPPG measurement scheme is the environment noisy, which are consisted of the white noisy of the camara, the unbalanced illumination, transparency difference of the subjects' skin, and etc. Therefore, the ICA, PCA, etc.[15]–[19] were often used to filter the original data in many studies. These algorithms work well in many scenes, but when the illuminance changes drastically, the measurement accuracy of these algorithms drops significantly. To weaken the influence of illumination changes on the data, a method based on the absorption of different light by blood was proposed to reduce the noise.

After finishing the preprocessing of the video, we can obtain , , and . Where

is the number of frames of the images, is the sum values of ROI in red channel, is the sum values of ROI in green channel, is the sum values of ROI in blue channel.

When the environmental light changes, the RGB value changes as well. If there is a sharp change in the environmental light, the noise may be much larger than the heart rate signal leading to the failure of obtaining the heart rate. Studies shown that blood hardly absorbs any red light [20][21], which indicates that changes in the red value reflect environmental light changes [22]–[24].We proposed a filtering method by calculating the difference of R and G value to reduce the noise from changes in environmental light. The noise is eliminated by subtracting the G value from the R value and the filtered signal represents as

Where is the filtered signal, is the area of the measurement area. And the experiments shown that this formula works best other formulas, which are well illustrated by Fig.3. After the operations above, the video were convert into signal which show the best SNR. The following operations were performed based on signal .

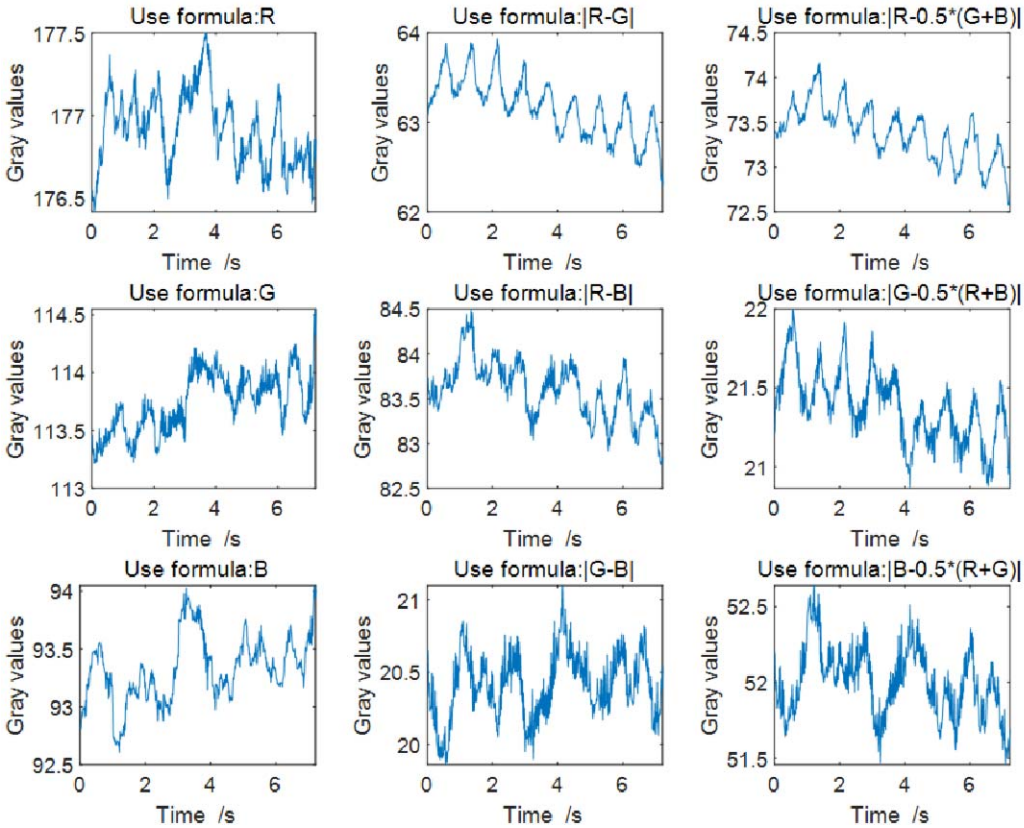

Fig.3 The gray value change curve obtained by using different formulas

C. Fast Fourier transform(FFT) for heart rate measurement

After fliting the noisy by subtracting the G value from the R value, we need calculated the heart rate from the filtered data $h_{(k)}$. Fast Fourier transform(FFT) is used to obtain the vector spectrum of the heart rate signal. The specific formulas of FFT are Eq.2 and Eq.3.

$$Y(k) = \sum_{j=1}^{n} h(j) W_n^{(j-1)(k-1)} \#(2)$$

$$W_n = e^{\frac{-2\pi i}{n}} \#(3)$$

Where n is resolution of FFT, $Y(k)$ is a vector sequence obtained after FFT. Perform modulo operation on $Y(k)$ to obtain $M(k)$ (The frequency domain data of the filtered signal).The filtered signal in frequency domain represents as $M(k) = |Y(k)|$.

After the above operations, we convert the filtered signal $h_{(k)}$ (time domain signal) into $M(k)$ (frequency domain signal). $M(k)$ shows the amount of signal (Bd) in each given frequency band within a frequency range. The physiological range of human heart rate is between 40 and 220 beats per minute (bpm) [25]. So we set 40bpm as Hr_L and 220bpm as Hr_H. Then, heart rates value over Hr_H and below Hr_L are deleted as noise in the measured frequency domain signal. The frequency domain signal $M(k)$ at this time becomes $M(k)$ $(Hr_L < k < Hr_H)$. We look for the maximum value of $M(k)$ between Hr_L and Hr_H as the heart rate measured by rPPG.

D. Searching ROI

Using the above operation, we can get the heart rate of the ROI, but it does not explain how to select the ROI. A suitable ROI contains more signals and less noisy. Therefore, searching a good ROI will greatly increase the SNR, improve the detection accuracy and even extend the detection distance. There are mainly two methods for selecting ROI. One is to set the entire skin as ROI [15]. This method can reduce the calculation burden of the device, but it also can weak the overall SNR by bring many parts with low signal content into the measurement area. The other one is to select the position with more blood vessels on the skin as the ROI [17], [21]. But which place is the mostly efficiency parts for the heart rate detection have not been demonstrated. In this paper, we investigated the SNR map of the palm of five subjects of different gender and occupation as shown in Fig. 4.

Take the calculation of the heart rate signal content ratio of a pixel as an example:

First, we use Eq.4 to collect the filtered data $h(k)$ of this pixel. Where k is the number of frames of the images, $R(k)$ is the sum values of ROI in red channel, $G(k)$ is the sum values of

ROI in green channel.

Secondly, we use Eq.2 , Eq.3, and to perform fast Fourier transform on the signal of this pixel to obtain the content (dB) of the signal in different frequency domains .

Thirdly, use Eq.5 to calculate the average value of the frequency domain signal from to .

Fourthly, use ECG to obtain the true heart rate of the test subject in the video, and use Eq.6 to calculate the SNR.

Finally, use the above method to calculate the SNR of each pixel. We use colors to indicate different SNR and draw them (Fig.4). In order to show the signal strength more clearly, we use black for pixels with SNR lower than 0, and red for pixels with SNR higher than 6. It is obviously that the best SNR is the most frequently occurred in the area marked by white square. Therefore, this area is selected as ROI. Although, there may be not contains the most vascular according to the anatomy of the palm as shown in Fig.3B. The size of this area is about 5% of the whole palm.

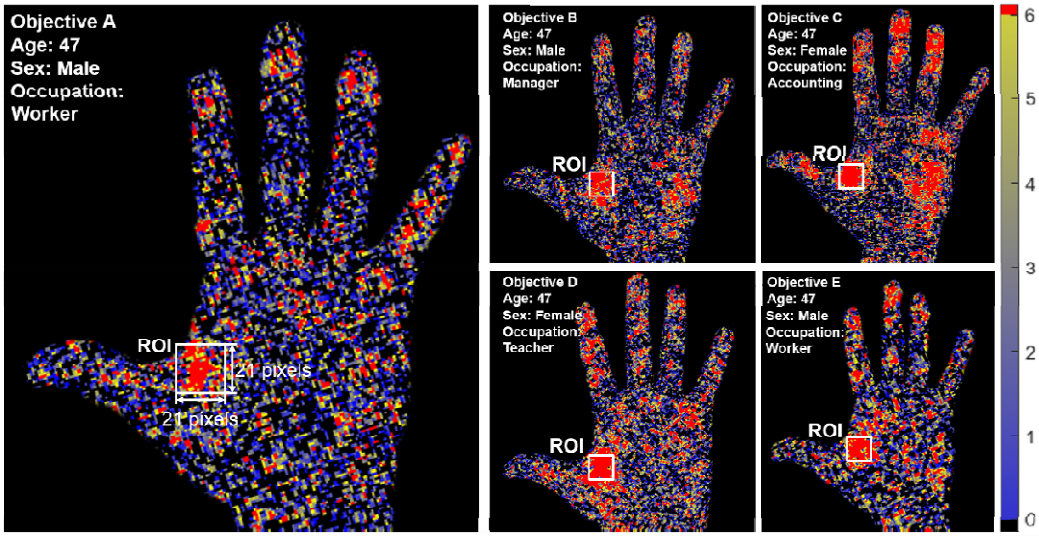

Fig.4 SNR map of the palm of five subjects of different gender and occupation.

Ⅲ. Result and Discussion

A. Result

Utilizing the methods mentioned above, we analyzed the hand video shown in Fig.2, which was shot at a distance of 4.8 meters at the illuminance of 250 Lux (easy office work illuminance [26]).

The results of each operation based on our method were well illustrated in Fig.5. The waveforms in Fig.5A shown the average intensity changes of pixels in ROI within 10 consecutive heartbeat cycles. However, it is very hard to show the periodicity of the heart rate from this result. While after fliting by subtracting the G value from the R value, the filtered signal well described the periodicity of the heart rate as shown in Fig.5B. Especially when comparing the ECG data in Fig.5C, we can obviously find that the periodicity of our results coincides with that of the ECG result. To show this point more clearly, the signal amplitude of ECG and rPPG results at different frequencies are calculated and compared using the FFT algorithm in Fig.5D. The coincided peaks of the two waveforms obtained by these two kinds of methods demonstrated that the heart rate measured by our rPPG methods is as correct as that of ECG.

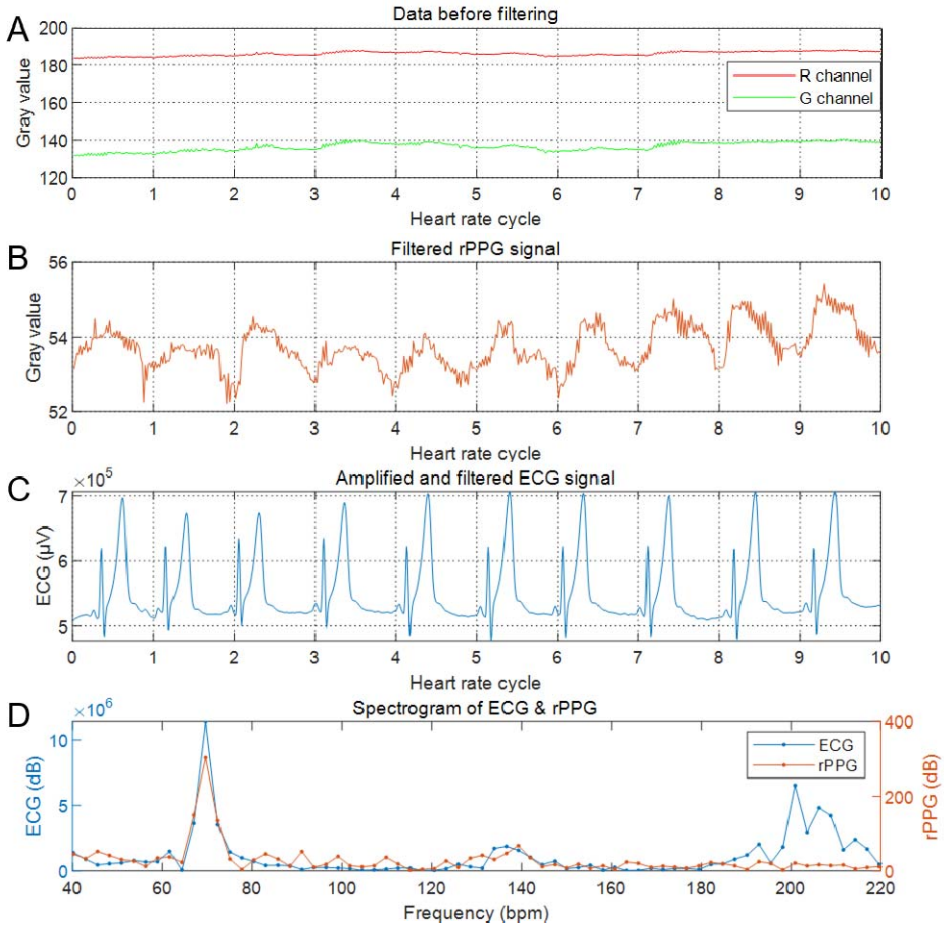

Fig.5 Waveform of the data measured by rPPG before (**A**) and after (**B**) filtering; (**C**) Waveform of the data measured by ECG after filtering; (**D**) Using FFT to analyze the data measured by rPPG and ECG to obtain the amplitude distribution of waves of different frequencies;

B. Measuring accuracy with illuminance

To explore the effects of illuminance on the experimental results, 7 more experiments were carried out in different lighting conditions 3.1 meters away from the same subject. The illuminance in the 7 groups of experiments were controlled with the range of 283.5-284.3 Lux (normal office lighting [28]), 100.3-101.4 Lux (dark overcast day[26], [29]), 52.4-53.5 Lux (living room lights [28]), 32.4-32.5 Lux, 14.8-16.8 Lux (dark surroundings), 9.8-10.8 Lux (twilight), and 3.4-3.5 Lux. Fig.6 shows that the measurement accuracy rises with the increase of illuminance in an exponential way and reached 96.71% when the illuminance increased to 32.4 Lux. When the illuminance increased to 100.03 Lux, the measuring accuracy increased slowly and reached a plateau ~ 99.99%.

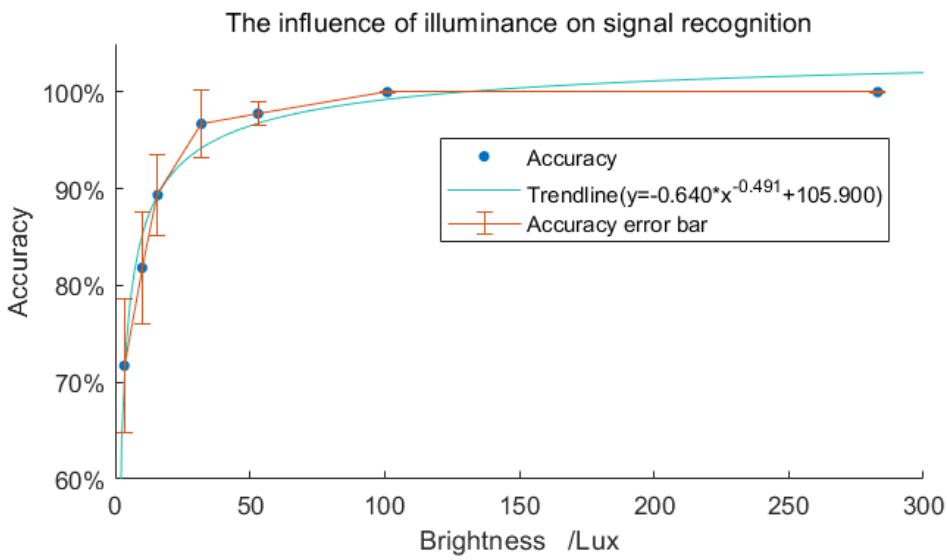

Fig.6 The influence of illuminance on signal recognition.

C. Light robustness verification

To evaluate the light robustness and reliability of our rPPG methods, we performed this verification experiments by introducing two kinds of light noises of sudden increase and decrease of illuminance 3.1 meters away from the same subject. Which are two types of environment light interference: 1) illuminance drops suddenly (illumination reduced from 1000 Lux to 100 Lux), and 2) illuminance increases suddenly (illumination increased from 100 Lux to 1000 Lux).

Fig.7 shows gray values of R & G before filtering and the data after filtering. The signal before filtering also changes drastically when the illuminance changes. We cannot directly observe periodic changes from the signal before filtering. The filtered signal can clearly observe the

periodic change, and the change is little affected by the change in illuminance. This experiment proves that our method has strong illumination robustness.

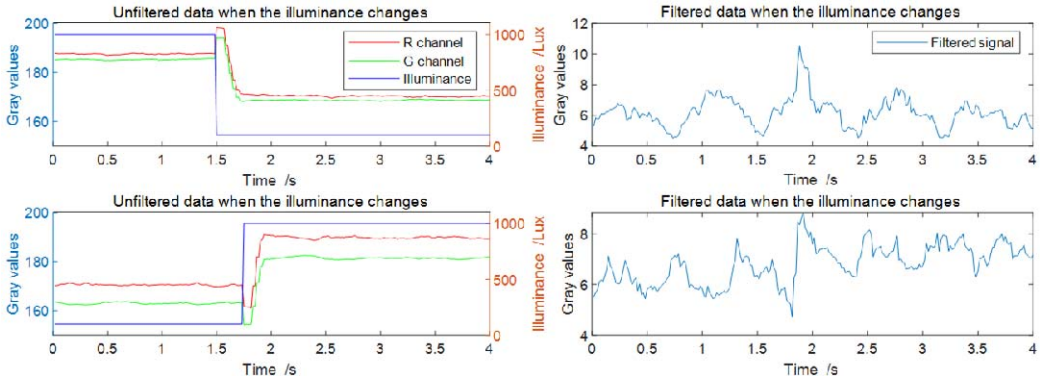

Fig.7 Data under changes in illuminance

Tab.2 The influence of noise

Ambient light intensity /Lux	Accuracy	Standard deviation of accuracy
100	99.99%	0.01
1000	99.99%	0.01
1000→100	99.99%	0.01
100→1000	99.99%	0.01

D. Measuring accuracy with distance

To verify the influence of the distance between camera and subject, we performed a serial experiments. The environmental light (250Lux, easy office work illuminance [26]) of these 11 groups are the same, while measurement distances are settled as 0cm, 50cm, 100cm, 150cm, 200cm, 240cm, 320cm, 400cm, 480cm, 560cm and 640cm respectively.

Fig.8 shows that the measurement accuracy decreases with the measurement distance. When the experimental distance increased to 320cm, the accuracy remains over 99.99%. When the distance increases to 480cm, the accuracy decreased slowly but still keep a high accuracy (over 97.09%). However, when the distance is over 560cm, the camera's sensitivity and resolution reduced greatly, then the camera cannot capture the small changes in skin color. Therefore, the measurement accuracy for the heart rate drops sharply to 90.12%.

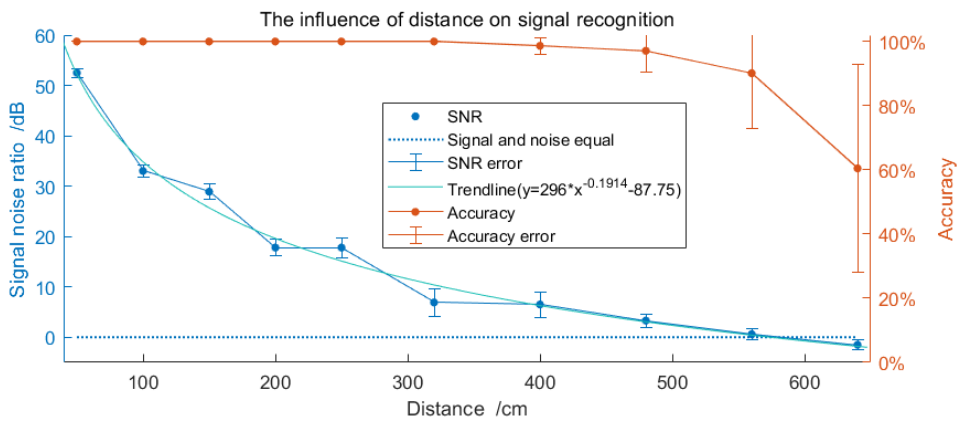

Fig.8 The influence of distance on signal recognition and signal noise ratio. (Each experiment with a distance of 4.8 meters was carried out 5 times, the experiment with a distance of 4.8 meters was carried out 7 times, the experiment with a distance of 5.6 meters was carried out 12 times, and the experiment with a distance of 6.4 meters was carried out 14 times.)

Ⅳ. Future work

In future works, We will use surveillance cameras with infrared functions for data collection, and shift the focus of research to near-infrared light filtering and data analysis. We will focus on multi-person heart rate measurement on remote monitors in public. The filtering algorithm will be optimized to enable longer-distance measurement, and face tracking will be added to achieve multi-activity target ROI selection. We will cooperate with hospitals to collect data from a large number of patients and realize the prediction of some common cardiovascular diseases through deep learning.

Ⅴ. Conclusions

We found that many remote heart rate measurement methods require a more demanding lighting environment, and the measurement distance is shorter. We use R channel minus G channel method to detect the relative value of the gray value change in the ROI area, and use TTF to obtain the heart rate. The combination of these two methods can greatly reduce the impact of illumination changes on the results. We use the above method to calculate the SNR of each pixel in the video, and find the area with the largest SNR as the ROI. This greatly weakens the need for illuminance and extends the measurement distance.

We measured the heart rate at a distance of 4.8 meters under a stable and sufficient light (250 Lux), and got the same result as the result measured by ECG. The measurement accuracy will change as the measurement distance and illumination change. We set up an illuminance control

group and a distance control group, and obtained the relationship between these two variables and the measurement accuracy. We let the environment brightness switch between low illumination and high illumination. We analyze the filtered data and the results verify that our method has strong illumination robustness.

The method in this study can be used to measure the heart rate with an ordinary camera, non-invasive, non-contact, avoiding the discomfort of the traditional measurement method to the testee, and easy to operate, low cost, and can be used for daily heart rate monitoring. Apply the method proposed in this study to the family. Using the home-installed surveillance network camera, you can observe the user's heart rate in real time and calculate the possibility of the user suffering from cardiovascular disease. When the probability of illness is higher than a certain value, the user is reminded to go to the hospital for examination in time. It has important value for the prevention of cardiovascular diseases. This method can also be applied to areas such as nursing homes, offices, dormitories, etc.

Reference

[1] Z. Zhang, Z. Pi, and B. Liu, "TROIKA: A general framework for heart rate monitoring using wrist-type photoplethysmographic signals during intensive physical exercise," *IEEE Trans. Biomed. Eng.*, vol. 62, no. 2, pp. 522–531, 2015, doi: 10.1109/TBME.2014.2359372.

[2] M. Adam, J. Krãmer, and C. Weinhardt, "Excitement up! Price down! Measuring emotions in Dutch auctions," *Int. J. Electron. Commer.*, vol. 17, no. 2, pp. 7–40, 2012, doi: 10.2753/JEC1086-4415170201.

[3] P. J. Astor, M. T. P. Adam, P. Jerčić, K. Schaaff, and C. Weinhardt, "Integrating biosignals into information systems: A NeuroIS tool for improving emotion regulation," *J. Manag. Inf. Syst.*, vol. 30, no. 3, pp. 247–278, 2013, doi: 10.2753/MIS0742-1222300309.

[4] R. M. Carney, K. E. Freedland, P. K. Stein, J. A. Skala, P. Hoffman, and A. S. Jaffe, "Change in heart rate and heart rate variability during treatment for depression in patients with coronary heart disease," *Psychosom. Med.*, vol. 62, no. 5, pp. 639–647, 2000, doi: 10.1097/00006842-200009000-00007.

[5] G. Mancia *et al.*, "Blood pressure and heart rate variabilities in normotensive and hypertensive human beings," *Circ. Res.*, vol. 53, no. 1, pp. 96–104, 1983, doi: 10.1161/01.RES.53.1.96.

[6] M. Böhm *et al.*, "Heart rate as a risk factor in chronic heart failure (SHIFT): The association between heart rate and outcomes in a randomised placebo-controlled trial," *Lancet*, vol. 376, no. 9744, pp. 886–894, 2010, doi: 10.1016/S0140-6736(10)61259-7.

[7] C. B. Taylor, "Depression, heart rate related variables and cardiovascular disease," *Int. J. Psychophysiol.*, vol. 78, no. 1, pp. 80–88, 2010, doi: 10.1016/j.ijpsycho.2010.04.006.

[8] A. Cultur *et al.*, "Covariance structure analysis of health-related indicators in elderly people at home with a focus on subjective feeling of health," *Geographie*, vol. 18, no. April 2007, p. 2014, 2009.

[9] S. Petersen, V. Peto, M. Rayner, J. Leal, R. Luengo-Fernandez, and A. Gray, "European Cardiovascular Statistics: 2005 edition," pp. 1–25, 2005.

[10] M. Nichols, N. Townsend, and M. Rayner, "European cardiovascular disease statistics," *Eur. Hear. Netw. Eur. Soc. Cardiol.*, pp. 10–123, 2012.

[11] E. Wilkins, L. Wilson, K. Wickramasinghe, and P. Bhatnagar, "European Cardiovascular Disease Statistics 2017 edition," *Eur. Hear. Netw.*, pp. 94–100, 2017, [Online]. Available: www.ehnheart.org.

[12] "https://www.who.int/news-room/fact-sheets/detail/cardiovascular-diseases-(cvds)." .

[13] M. Lewandowska, J. Rumiński, T. Kocejko, and J. Nowak, "Measuring pulse rate with a webcam - A non-contact method for evaluating cardiac activity," *2011 Fed. Conf. Comput. Sci. Inf. Syst. FedCSIS 2011*, pp. 405–410, 2011.

[14] E. F. Greneker, "Radar sensing of heartbeat and respiration at a distance with applications of the technology," in *IEE Conference Publication*, 1997, no. 449, pp. 150–154, doi: 10.1049/cp:19971650.

[15] M. Z. Poh, D. J. McDuff, and R. W. Picard, "Advancements in noncontact, multiparameter physiological measurements using a webcam," *IEEE Trans. Biomed. Eng.*, vol. 58, no. 1, pp. 7–11, 2011, doi: 10.1109/TBME.2010.2086456.

[16] D. Djeldjli, F. Bousefsaf, C. Maaoui, and F. Bereksi-Reguig, "Imaging Photoplethysmography: Signal Waveform Analysis," *Proc. 2019 10th IEEE Int. Conf. Intell. Data Acquis. Adv. Comput. Syst. Technol. Appl. IDAACS 2019*, vol. 2, pp. 830–834, 2019, doi: 10.1109/IDAACS.2019.8924239.

[17] R. H. Goudarzi, S. Somayyeh Mousavi, and M. Charmi, "Using imaging Photoplethysmography (iPPG) Signal for Blood Pressure Estimation," *Iran. Conf. Mach. Vis. Image Process. MVIP*, vol. 2020-Febru, pp. 14–19, 2020, doi: 10.1109/MVIP49855.2020.9116902.

[18] F. Wurtenberger, T. Haist, C. Reichert, A. Faulhaber, T. Boettcher, and A. Herkommer, "Optimum Wavelengths in the near Infrared for Imaging Photoplethysmography," *IEEE Trans. Biomed. Eng.*, vol. 66, no. 10, pp. 2855–2860, 2019, doi: 10.1109/TBME.2019.2897284.

[19] W. Verkruysse, L. O. Svaasand, and J. S. Nelson, "Remote plethysmographic imaging using ambient light," *Opt. Express*, vol. 16, no. 26, p. 21434, 2008, doi: 10.1364/oe.16.021434.

[20] W. G. Zijlstra, A. Buursma, and W. P. Meeuwsen-van der Roest, "Absorption spectra of human fetal and adult oxyhemoglobin, de-oxyhemoglobin, carboxyhemoglobin, and methemoglobin," *Clin. Chem.*, vol. 37, no. 9, pp. 1633–1638, 1991, doi: 10.1093/clinchem/37.9.1633.

[21] S. Sanyal and K. K. Nundy, “Algorithms for Monitoring Heart Rate and Respiratory Rate From the Video of a User’s Face,” *IEEE J. Transl. Eng. Heal. Med.*, vol. 6, no. February, pp. 1–11, 2018, doi: 10.1109/JTEHM.2018.2818687.

[22] G. De Haan and V. Jeanne, “Robust pulse rate from chrominance-based rPPG,” *IEEE Trans. Biomed. Eng.*, vol. 60, no. 10, pp. 2878–2886, 2013, doi: 10.1109/TBME.2013.2266196.

[23] “M. Huelsbusch, ‘Ein bildgestuetstes, funktionelles Verfahren zur optoelektronischer Erfassung der Hautperfusion,’ Ph.D. dissertation, Fakultaet fuer Elektrotechnik un Informationstechnik, RWTH Aachen Univ., Aachen, Germany, p. 70, Jan. 28, 2008.” .

[24] Y. C. Lin and Y. H. Lin, “A study of color illumination effect on the SNR of rPPG signals,” *Proc. Annu. Int. Conf. IEEE Eng. Med. Biol. Soc. EMBS*, pp. 4301–4304, 2017, doi: 10.1109/EMBC.2017.8037807.

[25] “K. Otsuka et al., ‘Circadian period of human blood pressure and heart rate in clinical health under ordinary conditions,’ [1989] Proceedings. Second Annual IEEE Symposium on Computer-based Medical Systems, Minneapolis, MN, USA, 1989, pp. 206-213, doi: 10.”

[26] S. Di Pilla, “U.S. Standards and Guidelines,” *Slip, Trip, Fall Prev.*, pp. 161–194, 2009, doi: 10.1201/9781420082364.ch5.

[27] A. Yunitsyna, “Universal Space in Dwelling–the Room for All Living Needs,” no. 131, pp. 8–10, 2014.

[28] A. Pears, “Strategic Study of Household Energy and Greenhouse Issues a Report for Environment Australia,” *Solutions*, no. June, pp. 1–110, 1998.

[29] “Schlyter, P. . (2010). Radiometry and photometry in astronomy. Retrieved October.” .

[30] “Electro-Optics Handbook . photonis.com. p. 63. Retrieved 2 April 2012.” .

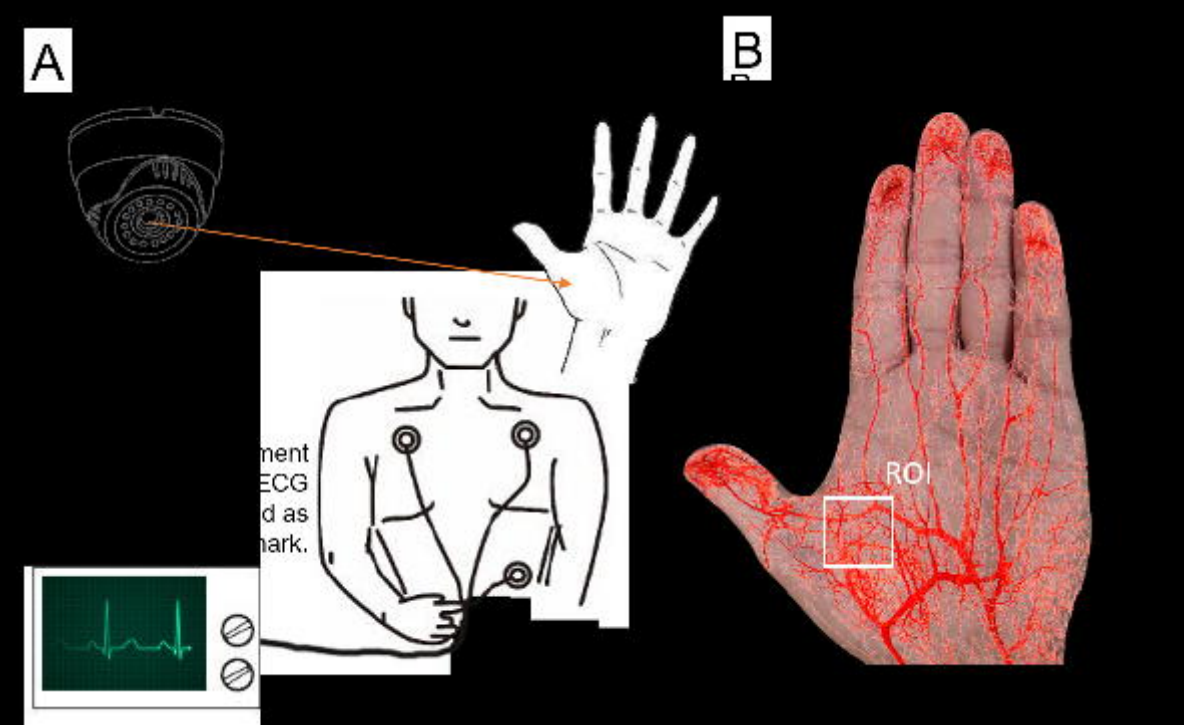
A
B
ROI

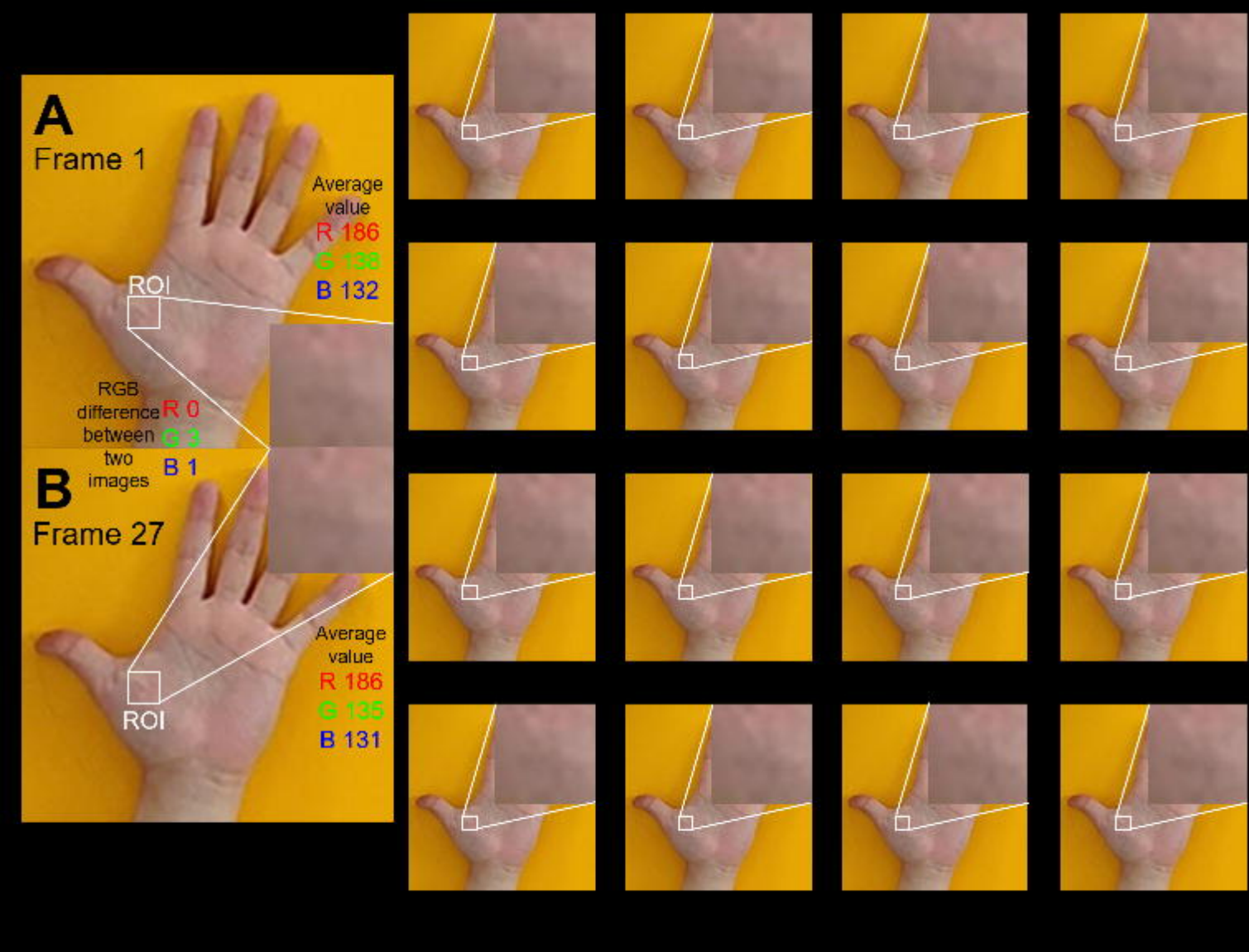
A
Frame 1
Average value
R 186
G 138
B 132
ROI
RGB difference between two images
R 0
G 3
B 1
B
Frame 27
Average value
R 186
G 135
B 131
ROI

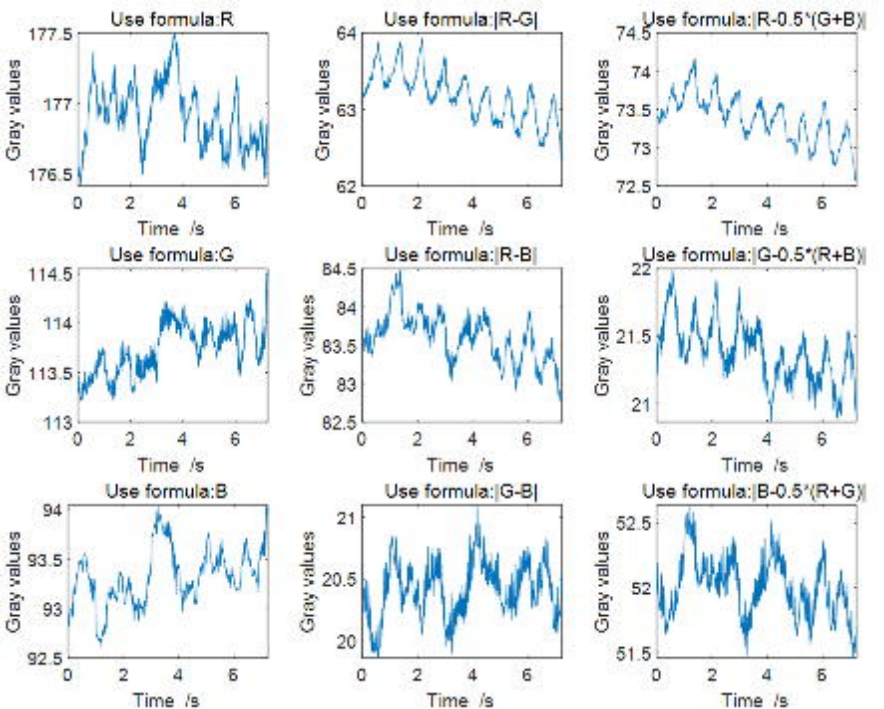
Use formula:R
Use formula:|R-G|
Use formula:|R-0.5*(G+B)|
Use formula:G
Use formula:|R-B|
Use formula:|G-0.5*(R+B)|
Use formula:B
Use formula:|G-B|
Use formula:|B-0.5*(R+G)|
Gray values
Time /s

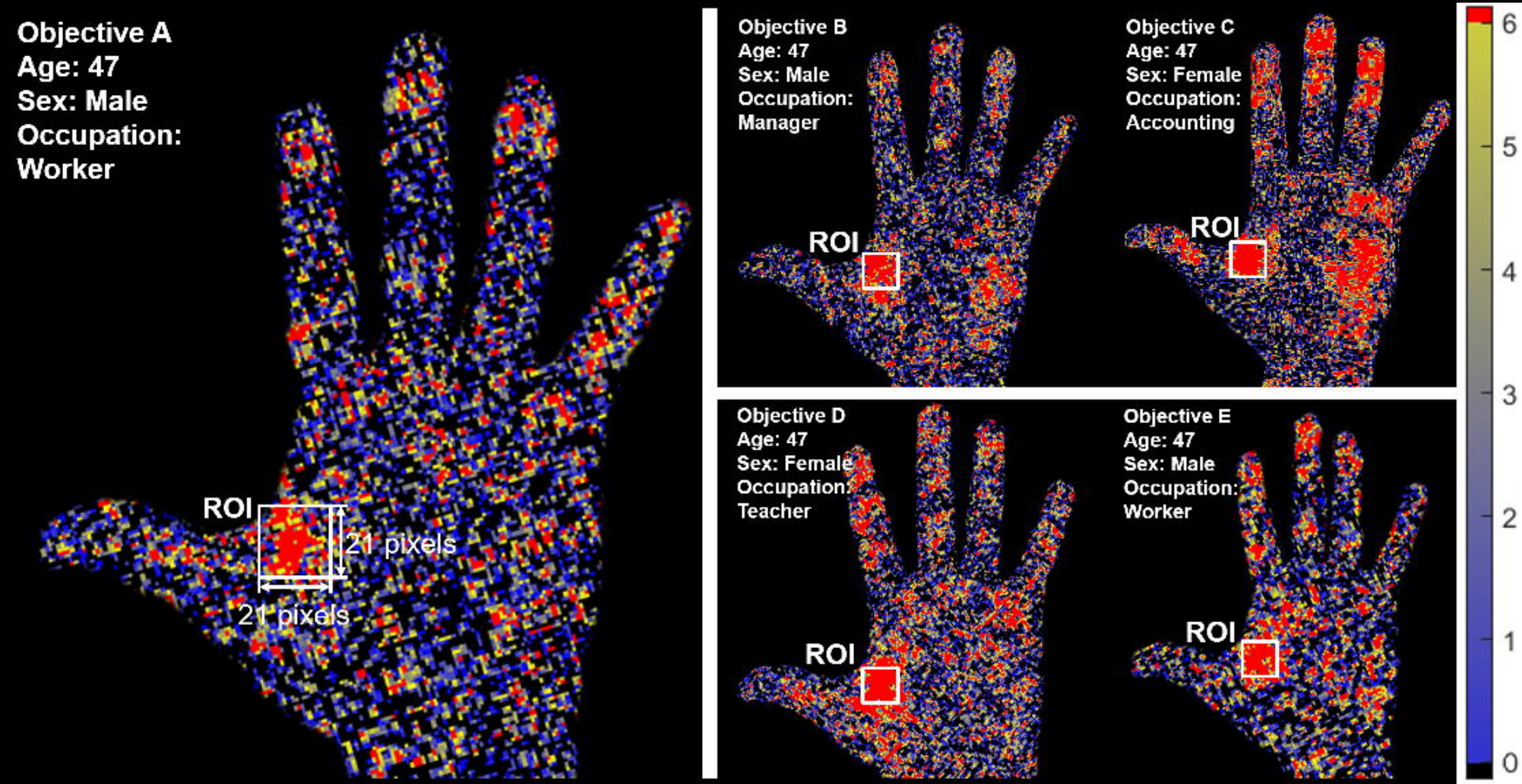
Objective A
Age: 47
Sex: Male
Occupation:
Worker
ROI
21 pixels
21 pixels
Objective B
Age: 47
Sex: Male
Occupation:
Manager
ROI
Objective C
Age: 47
Sex: Female
Occupation:
Accounting
ROI
Objective D
Age: 47
Sex: Female
Occupation:
Teacher
ROI
Objective E
Age: 47
Sex: Male
Occupation:
Worker
ROI
6
5
4
3
2
1
0

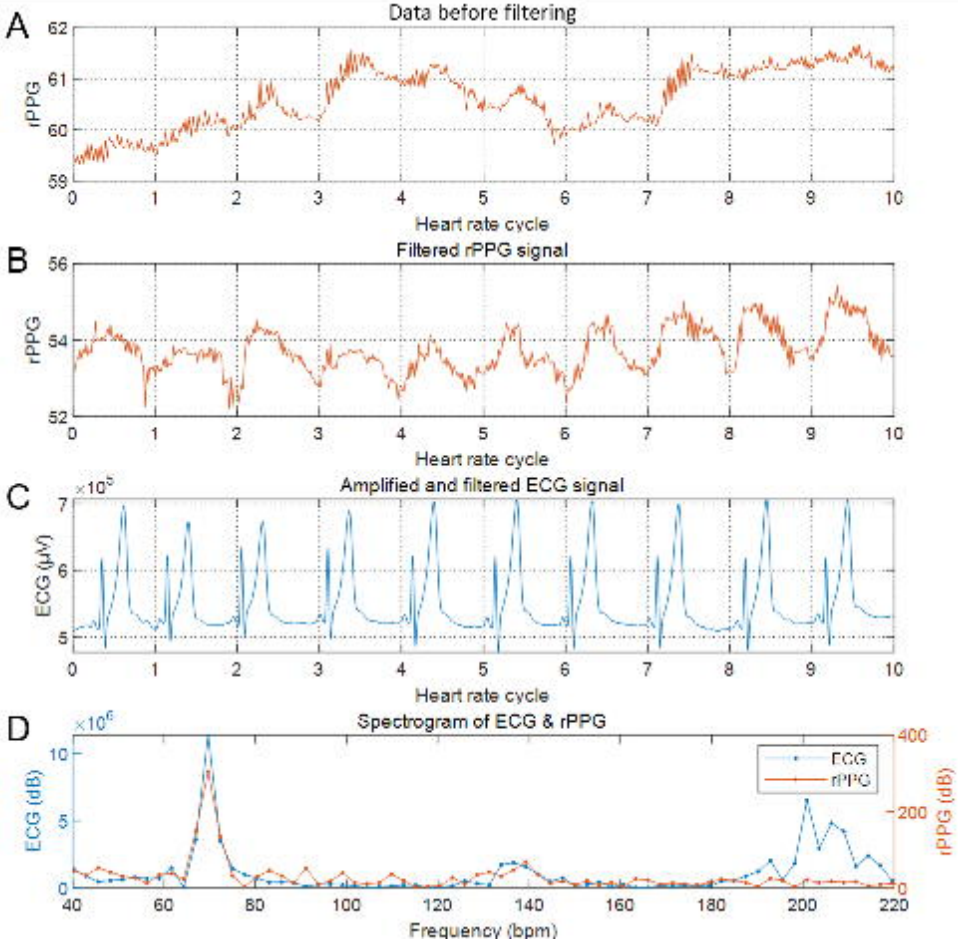
A
Data before filtering
rPPG
Heart rate cycle
B
Filtered rPPG signal
rPPG
Heart rate cycle
C
Amplified and filtered ECG signal
ECG (μV)
Heart rate cycle
D
Spectrogram of ECG & rPPG
ECG (dB)
rPPG (dB)
ECG
rPPG
Frequency (bpm)

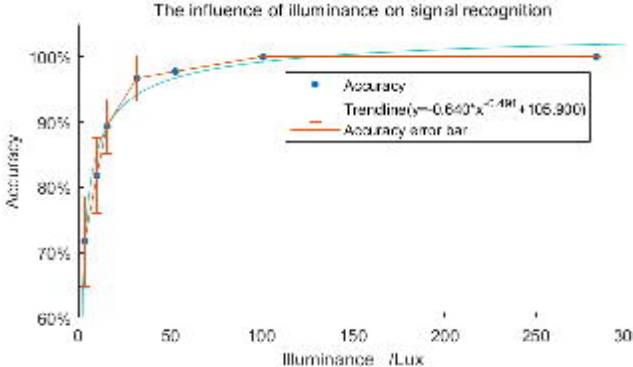
The influence of illuminance on signal recognition
100%
90%
80%
70%
60%
Accuracy
0
50
100
150
200
250
300
Illuminance /Lux
Accuracy
Trendline(y=-0.640*x^-0.481+106.900)
Accuracy error bar

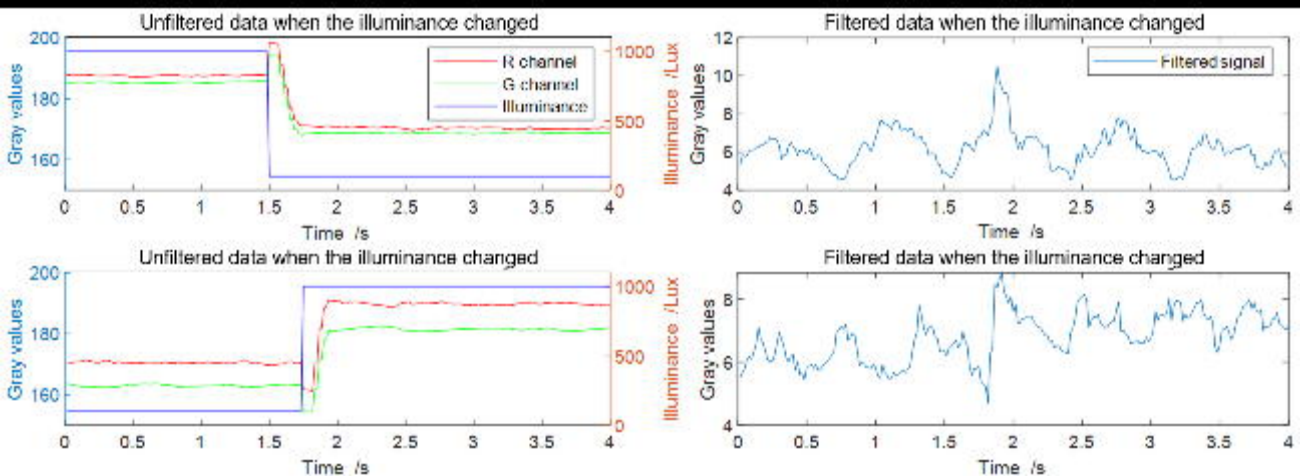
Unfiltered data when the illuminance changed
Gray values
Illuminance /Lux
Time /s
R channel
G channel
Illuminance
Filtered data when the illuminance changed
Filtered signal
Unfiltered data when the illuminance changed
Filtered data when the illuminance changed

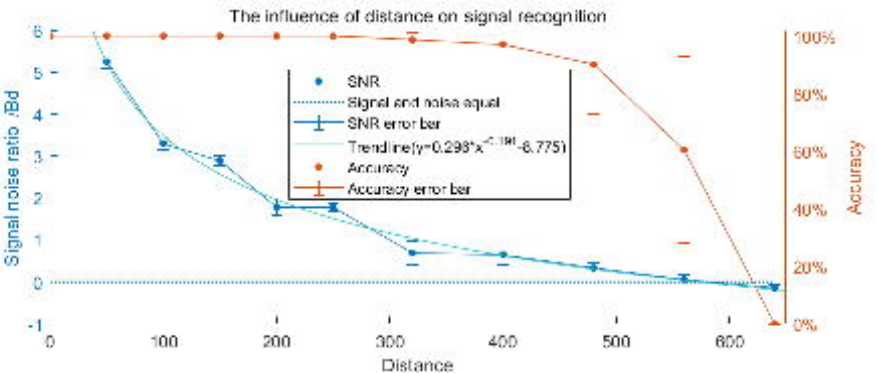
The influence of distance on signal recognition
Signal noise ratio /Bd
Accuracy
Distance
SNR
Signal and noise equal
SNR error bar
Trendline(y=0.293*x^-1.191-8.775)
Accuracy
Accuracy error bar
6
5
4
3
2
1
0
-1
100%
80%
60%
40%
20%
0%
0
100
200
300
400
500
600

Core algorithm	Shooting time /second	Research on brightness robustness Y/N	Research on illumination range Y/N	Measuring range /meter	Study
ICA	60	N	N	0.5	[15]
PCA	30	N	N	1	[13]
Butterworth pass band filter	60	N	N	<3	[16]
RTR	35	N	N	1	[17]
FFT	30	N	N	0.8-1	[18]
FFT	30	N	N	1-2	[19]
Filtering for blood color +FFT	20	Y	Y	<4.8	This study

Ambient light intensity /Lux	Accuracy	Standard deviation of accuracy
100	99.99%	0.01
1000	99.99%	0.01
1000→100	99.99%	0.01
100 →1000	99.99%	0.01

Ambient light intensity /Lux	Accuracy	Standard deviation of accuracy
283.5~284.3	99.99%	0.01
100.3~101.4	99.99%	0.01
52.4~53.5	97.76%	1.18
32.4~32.5	96.71%	3.54
14.8~16.8	89.35%	4.21
9.8~10.8	81.82%	5.77
3.4~3.5	71.72%	6.88

Distance /cm	Accuracy	Standard deviation of accuracy	SNR	Standard deviation of SNR
50	99.99%	0.01	5.25	0.09
100	99.99%	0.01	3.30	0.12
150	99.99%	0.01	2.89	0.16
200	99.99%	0.01	1.78	0.16
250	99.99%	0.01	1.78	0.20
320	99.99%	0.01	0.69	0.28
400	98.65%	2.53	0.65	0.25
480	97.09%	6.58	0.33	0.13
560	90.12%	17.12	0.06	0.10
640	60.47%	32.30	-0.15	0.09